

# INFRARED AND OPTICAL OBSERVATIONS OF GRB 030115 AND ITS EXTREMELY RED HOST GALAXY: IMPLICATIONS FOR DARK BURSTS<sup>1</sup>

ANDREW LEVAN<sup>2,3</sup>, ANDREW FRUCHTER<sup>3</sup>, JAMES RHOADS<sup>3</sup>, BAHRAM MOBASHER<sup>3</sup>, NIAL TANVIR<sup>4</sup>, JAVIER GOROSABEL<sup>3,5</sup>, EVERT ROL<sup>2,6</sup>, CHRYSOA KOUVELIOTOU<sup>7</sup>, IAN DELL'ANTONIO<sup>8,9</sup>, MICHAEL MERRILL<sup>10</sup>, EDDIE BERGERON<sup>3</sup>, JOSÉ MARÍA CASTRO CERÓN<sup>3</sup>, NICOLA MASETTI<sup>10</sup>, PAUL VREESWIJK<sup>11</sup>, ANGELO ANTONELLI<sup>12</sup>, DAVID BERSIER<sup>3</sup>, ALBERTO CASTRO-TIRADO<sup>5</sup>, JOHAN FYNBO<sup>13</sup>, PETER GARNAVICH<sup>14</sup>, STEPHEN HOLLAND<sup>15</sup>, JENS HJORTH<sup>16</sup>, PETER NUGENT<sup>17</sup>, ELENA PIAN<sup>18</sup>, ALAIN SMETTE<sup>19</sup>, BJARNE THOMSEN<sup>11</sup>, STEPHEN E. THORSETT<sup>20</sup>, RALPH WIJERS<sup>6</sup>

*Draft version October 1, 2018*

## ABSTRACT

We present near-infrared (nIR) and optical observations of the afterglow of GRB 030115. Discovered in an infrared search at Kitt Peak 5 hours after the burst trigger, this afterglow is amongst the faintest observed in the R-band at an early epoch, and exhibits very red colors, with  $R-K \approx 6$ . The magnitude of the optical afterglow of GRB 030115 is fainter than many upper limits for other bursts, suggesting that without early nIR observations it would have been classified as a “dark” burst. Both the color and optical magnitude of the afterglow are likely due to dust extinction and indicate that at least some optical afterglows are very faint due to dust along the line of sight. Multicolor *Hubble Space Telescope* observations were also taken of the host galaxy and the surrounding field. Photometric redshifts imply that the host, and a substantial number of faint galaxies in the field are at  $z \sim 2.5$ . The overdensity of galaxies is sufficiently great that GRB 030115 may have occurred in a rich high-redshift cluster. The host galaxy shows extremely red colors ( $R-K=5$ ) and is the first GRB host to be classified as an Extreme Red Object (ERO). Some of the galaxies surrounding the host also show very red colors, while the majority of the cluster are much bluer, indicating ongoing unobscured star formation. As it is thought that much of high redshift star formation occurs in highly obscured environments it may be that GRB 030115 represents a transition object, between the relatively unobscured afterglows seen to date and a population which are very heavily extinguished, even in the nIR.

*Subject headings:* gamma rays: bursts

## 1. INTRODUCTION

Most ground-based GRB afterglow searches are being pursued first in optical wavelengths. These have relied on either comparing a newly acquired image to an archival image (normally the Digitized Sky Survey) and locating any new sources, or on performing multi-epoch observations and identifying any variable sources within the GRB error box. In many cases both approaches have been used. Such searches have resulted in the discovery of approximately 60 GRB afterglows with about 50% and 35% being discovered, respectively, by each of the methods, and  $\sim 15\%$  being discovered by a combination thereof. One GRB afterglow was found by a color-color technique, (Rhoads 2001; Gorosabel *et al.* 2002), exploiting the ability of multi-band observations to distinguish blackbody stellar spectra from the power-law spectra displayed by GRB afterglows.

The advent of small robotic telescopes that can slew automatically in response to GRB alert notices (e.g., ROTSE) and larger telescopes that can easily be remotely operated (e.g., the Palomar 48 inch) has increased the discovery rate of young and bright afterglows. For example, the afterglows of GRB 021004 and GRB 021211 were discovered only minutes after the GRB trigger (Fox 2002; Fox *et al.* 2003a,b). These rapid-response cam-

34131 Trieste, Italy

<sup>19</sup> Institut d’Astrophysique et de Géophysique, Université de Liège, Avenue de Coïnte, 5, B-4000 Liège, Belgium

<sup>20</sup> Department of Astronomy and Astrophysics, University of California, 1156 High Street, Santa Cruz, CA 95064, USA

<sup>1</sup> Based in part on observations made with the NASA/ESA *Hubble Space Telescope*, obtained at the Space Telescope Science Institute, operated by the Association of Universities for Research in Astronomy, Inc., under NASA contract NAS 5-26555. These observations are associated with programs 9074 and 9405.

<sup>2</sup> Department of Physics and Astronomy, University of Leicester, University Road, Leicester, LE1 7RH, UK

<sup>3</sup> Space Telescope Science Institute, 3700 San Martin 7 Drive, Baltimore, MD21218, USA

<sup>4</sup> Centre for Astrophysics Research, University of Hertfordshire, College Lane, Hatfield, Hertfordshire, AL10 9AB, UK

<sup>5</sup> Instituto de Astrofísica de Andalucía (IAA-CSIC), P.O. Box 03004, E-18080 Granada, Spain.

<sup>6</sup> Astronomical Institute, University of Amsterdam, Kruislaan 403, 1098 SJ Amsterdam, The Netherlands

<sup>7</sup> NASA/MSFC, NSSTC, XD-12, 320 Sparkman Drive, Huntsville, AL 35805, USA

<sup>8</sup> Physics Department, Brown University, Providence, RI 02912, USA

<sup>9</sup> National Optical Astronomy Observatory, P.O. Box 26732, Tucson, AZ 85726-6732, USA

<sup>10</sup> Istituto di Astrofisica Spaziale e Fisica Cosmica - Sezione di Bologna, CNR, via Gobetti 101, 40129, Bologna, Italy

<sup>11</sup> European Southern Observatory, Casilla 19001, Santiago 19, Chile

<sup>12</sup> Osservatorio Astronomico di Roma, Via Frascati 33, Monteporzio I-00040, Italy.

<sup>13</sup> Department of Physics and Astronomy, Aarhus University, Ny Munkegade, DK-8000, Aarhus, Denmark

<sup>14</sup> Department of Physics, University of Notre Dame, Notre Dame, IN 46556-5670, USA

<sup>15</sup> US Naval Observatory, Flagstaff Station, P.O. Box 1149, Flagstaff, AZ 86002, USA

<sup>16</sup> Astronomical Observatory, University of Copenhagen, Juliane Maries Vej 30, DK-2100, Copenhagen, Denmark

<sup>17</sup> Lawrence Berkeley National Laboratory, 1 Cyclotron Road, Berkeley, CA 94720, USA

<sup>18</sup> Osservatorio Astronomico di Trieste, Via G.B. Tiepolo 11,

paigns have also substantially decreased the fraction of bursts that have no identified optical counterparts: the so called “dark bursts.” Of the GRBs well localised so far by the Wide X-ray Monitor (WXM) on *HETE-2*, the optical counterpart discovery percentage is  $\sim 60\%$ , while for bursts localized by the Soft X-Ray Camera (SXC) the discovery rate is  $\sim 90\%$ , (largely due to the smaller error boxes associated with SXC positions - see for example, Lamb *et al.* 2003). There are evidently possible selection effects: relatively bright and soft bursts are more easily localised by the SXC, and these smaller error boxes are easier to search to deep limits. Indeed, although *Swift* now allows routine  $\sim 3$  arcminute error boxes to be routinely circulated its increased sensitivity means that it locates fainter bursts, and the recovery rate of optical afterglows is lower than for the SXC. Nevertheless the dark burst fraction does appear to have decreased significantly from the  $\geq 70\%$  that was typical during the first few years of GRB observations, when slow and less accurate positions made it more difficult to locate afterglows, even for relatively bright bursts (see e.g. Fynbo *et al.* 2001; Lazzati *et al.* 2002).

The spectral energy distribution (SED) of a GRB afterglow is best described by a set of connected power-laws with breaks due to synchrotron self-absorption, the peak energy of the electrons, and the time-dependent cooling of the fireball (Sari, Piran & Narayan 1998). In theory, knowledge of these break frequencies allows us to reconstruct details of the afterglow (as has been done for a number of well sampled GRB afterglows to-date, e.g., by Panaitescu & Kumar 2001). Theoretical models are also useful for studying GRBs with no optical afterglows, where observations in some bands (such as X-rays and radio) can be used to place limits on the expected optical flux. In a prototypical dark burst, such as GRB 970828 (Groot *et al.* 1998; Djorgovski *et al.* 2001), extrapolation of the X-ray flux, assuming a synchrotron spectrum, led to the conclusion that the burst should have been seen in the optical. Conversely, Fynbo *et al.* (2001) have shown that the classification of many bursts as dark may simply represent the failure to search either early or deep enough. This interpretation is supported by the detection of the faint afterglow of GRB 020124 (Berger *et al.* 2003) and the fast fading afterglow of GRB 021211 (Fox *et al.* 2003a; Crew *et al.* 2003), which would not have been detected but for early, deep observations. Although it is also true that the refinement of afterglow locations via X-ray observations does allow for very deep pointed observations, and thus enables faint afterglows to be located. This is now commonly the case for *Swift* bursts.

For the relatively small number of bursts that are still apparently “dark” despite deep and early optical limits, a number of plausible explanations have been widely discussed including i) bursts which occur at high- $z$  where the Lyman break has moved through the optical bands ii) GRBs which originate from behind significant obscuring columns, significantly attenuating the optical light, iii) bursts which are intrinsically faint (i.e. are spectrally similar to bright) afterglows but are a factor 10-100 fainter and iv) fade very rapidly so that, at the time of the first optical observations they have faded below the detection limit. Observations of afterglows to date, including recent observations of *Swift* bursts indicate that all of the above explanations may apply with some bursts

originating from beyond  $z=5$  (e.g. Jakobsson *et al.* 2005; Haislip *et al.* 2005; Kawai *et al.* 2005), a fraction being apparently obscured (e.g. De Pasquale *et al.* 2005; Watson *et al.* 2005). While the first two scenarios above have been used to motivate afterglow searches in the near-infrared, locating afterglows from bursts akin to the third and fourth options can be equally well done by early, deep optical observations.

As the connection between long-duration GRBs and supernovae is now secure (Hjorth *et al.* 2003; Stanek *et al.* 2003; Zeh, Klose & Hartmann 2004), we expect GRBs to point to locations of star formation throughout the Universe. The determination of which of the explanations above is the dominant origin of dark GRBs may thus shed light into the processes of star formation and its evolution. For example were many dark GRBs genuinely at high redshifts, they would point to strong star formation even at very early ages in the Universe, while if most are actually in obscured environments at lower redshifts they would support models whereby much of the star formation in the Universe is obscured. Moreover, the type of their host galaxies, their environments and relative frequencies may also indicate where much of the star formation occurs.

Here we present the nIR discovery of the afterglow of GRB 030115. This burst was heavily reddened with respect to a model power law SED and, in the optical, was the faintest GRB afterglow ever observed at similar epochs post-burst. We show that its host galaxy lies at moderate redshift and has very red colors ( $R-K \sim 5$ ). It is therefore likely that GRB 030115 was reddened due to high local extinction. Furthermore there is a significant overdensity of galaxies at the redshift of the GRB host possibly associated with the latter; this putative galaxy cluster is a mix of young, blue, star forming systems and red systems which are either dusty starburst systems or contain an older stellar population. This cluster, if confirmed, is the first associated with a GRB, and one of very few known at  $z > 2$ .

Throughout this paper we assume a  $\Lambda$ CDM cosmology with  $\Omega_\Lambda = 0.73$ ,  $\Omega_M = 0.27$  and  $H_0 = 72 \text{ km s}^{-1} \text{ Mpc}^{-1}$ .

## 2. OBSERVATIONS

GRB 030115 was detected by the *HETE-2* satellite on 2003 January 15 at 02:44 UT, with a duration of  $t_{90} = 17.8$  seconds (Kawai *et al.* 2003). The burst, classified as an X-ray Rich GRB<sup>21</sup>, was localised by both the WXM and SXC instruments with error circles of 5 and 2 arcmin radius, respectively. Early optical observations were acquired by several groups using 1-2 m class telescopes. Comparing these images with the Digitized Sky Survey revealed no new objects, placing an early ( $\Delta t = t_{\text{obs}} - t_0 \approx 2$  hour) limit on the magnitude of the afterglow at  $R = 21$  (Castro Tirado *et al.* 2003; Blake *et al.* 2003). We obtained data from the Kitt Peak National Observatory (KPNO) 5 and 9 hours after the GRB in the infrared (J,H,K) bands, comparison of which revealed a fading IR source in all filters (see §2.1). Following our announcement of the IR counterpart, a re-inspection of early optical images obtained at  $\Delta t=2$  hours revealed a marginal optical detection (Masetti *et al.* 2003a). Further IR observations were obtained by Vrba *et al.* (2003),

<sup>21</sup> see <http://space.mit.edu/HETE/Bursts/Data/>

Kato *et al.* (2003) and Dullighan *et al.* (2004) and confirmed the fading nature of the object, thus securing its association with GRB 030115. Early radio observations at 8.46 GHz (Berger & Frail, 2003) failed to detect the afterglow candidate at  $\Delta t=5$  hours, specifically recording a flux density of  $84 \pm 62 \mu\text{Jy}$ . However, further observations at  $\Delta t=55$  hours detected a weak source coincident with that of the afterglow, with a flux level of  $94 \pm 22 \mu\text{Jy}$  (Frail & Berger 2003). Radio observations were also undertaken at the Westerbork Synthesis Radio Telescope (WSRT) at 3 epochs between 1.5 and 12 days post-burst. Combining these data provided a  $\sim 4\sigma$  detection of the radio transient at 4.9 GHz (Rol & Wijers 2003). Sub-millimeter observations were pursued with the SCUBA array on the James Clark Maxwell Telescope (JCMT) at  $850 \mu\text{m}$  (Hoge *et al.* 2003) and the Max-Planck Millimeter Bolometer (MAMBO) and IRAM 30-m telescope at 1.2 mm (Bertoldi *et al.* 2003). These placed  $3\text{-}\sigma$  limits at  $850 \mu\text{m}$  and 1.2 mm of 6 mJy and 3 mJy, respectively. While these observations are relatively deep (for afterglow searches), and would have detected the host if it were very bright in the submm (cf., Smail *et al.* 2002), the few sub-mm detections of GRB host galaxies to-date (e.g., Barnard *et al.* 2003; Berger *et al.* 2003; Tanvir *et al.* 2004) have been at the 3 mJy level (at  $850 \mu\text{m}$ ), and so would not have been detected at these limits.

### 2.1. Infrared observations

Observations at the KPNO 2.1 m telescope were undertaken using the SQUID (Simultaneous Quad Infrared Imaging Device) which provides 4 simultaneous colours (J,H,K & L). The sensitivity in the nIR is significantly greater than that in the mid-infrared (L-band) and hence only the J, H and K images were used for our analysis. A first epoch of observations was obtained 5 hours after the burst, with a second taken after 9 hours.

A PSF matched image subtraction was performed (using the ISISII code (Alard & Lupton 2000)). This led to the discovery of a transient source, seen to fade in the J, H and K bands. Using the UCAC-2 catalog we find a celestial position of RA=11:18:32.63, Dec=+15:02:59.9, with a positional accuracy of  $0''.1$ . The discovery images are shown in Figure 1.

Further IR observations were taken with INGRID at the William Herschel Telescope (WHT), and the NOT-CAM on the Nordic Optical Telescope, both sited on La Palma, SOFI on the 3.6 m New Technology Telescope at the European Southern Observatory (ESO) La Silla site (J,H and K-band, 26 hours after burst), and finally at the Very Large Telescope (VLT, UT1) at ESO, Paranal, using the ISAAC array. All of these IR observations were reduced through the ORAC-DR pipeline (Cavanagh *et al.* 2003). A summary is given in Table 1.

### 2.2. Optical Observations of the GRB 030115 afterglow

Optical observations of the GRB 030115 error box were performed by several groups. However these observations failed to reveal any possible candidates in comparison with the Digitized Sky Survey (Castro-Tirado *et al.* 2003; Masetti *et al.* 2003; Flaccomio *et al.* 2003; Lamb *et al.* 2003). We obtained data with the 1.82 m Copernico Telescope (first described by Masetti *et al.* 2003). at  $\Delta t=2$  hours in poor seeing ( $\sim 2.5''$ ). The images were bias subtracted and flat fielded in IRAF using standard

methods. The data contain a weak ( $4\sigma$ ) detection of the transient at this epoch from which we determine  $R=21.8 \pm 0.3$ .

Further optical data were obtained at the VLT using the FORS2 instrument in V, R and I on 2003 January 16 ( $\Delta t=26$  hours) and in R and I on 2003 January 17, using FORS1. These data were also reduced with IRAF, and again summarised in table 1.

### 2.3. HST observations of the GRB 030115 host galaxy

GRB 030115 was first imaged with the *Hubble Space Telescope* (HST) on 2003 February 10. At this epoch we obtained images in F606W (broad V-R) and F814W(I) filters using the Advanced Camera for Surveys (ACS) Wide Field Camera (WFC) as well as in F160W(H) using NICMOS and the NIC3 camera. A second epoch of observations were acquired on 2003 April 24, in F814W(I) and F110W (J) filters. A final set of observations were obtained on 2003 June 16 and 20 in F435W (B) and F222M (K) filters, providing us with a complete set of B(V-R)IJHK photometry on the host galaxy of GRB 030115. The results of these observations are summarised in table 2 (a subset of these observations have also been presented by Dullighan *et al.* 2004).

The ACS data were ‘‘On-The-Fly’’ calibrated to produce flattened images. They were then drizzled (Fruchter & Hook 2002) onto an output grid with pixels 0.66 times the size of the native ACS pixel (this corresponds to  $\sim 0''.033$ ). The linear drop size (`pixfrac`) was set to one.

In order to estimate the contribution of the afterglow to the late HST observations we aligned and subtracted the two F814W epochs taken at  $\Delta t=26$  and 127 days respectively. Our VLT/ISAAC image, taken 2 days after the burst, was also aligned with the F814W image, using 22 point sources common to each frame, allowing us to locate the afterglow position to  $\sim 0''.05$  accuracy. At this position we determine a  $3\sigma$  upper limit for the afterglow flux of  $F_{814W(AB)} = 28.2$  (at  $\Delta t=26$  days). Based on the measured R-band magnitude of  $R=21.8$  at  $\Delta t=2$  hours and the optical slope of  $\alpha = -1.4$  we would predict that the afterglow should have had  $I \sim 31$  at the time of this observation and thus the non-detection is in accordance with what we would expect by extrapolation of the early decay. We conclude that all of our HST observations contain negligible afterglow contamination of the host.

An additional possible cause of contamination could occur due to a possible supernova. Supernovae spectra peak in the optical rest frame, which lies in the IR bands at our favoured redshift (see Section 3.1). We do not have multi-epoch IR observations to test directly via image subtraction, however the expected flux of even an extreme event like SN 1998bw at  $z \sim 2$  is  $< 0.05 \mu\text{Jy}$  ( $F_{160W(AB)} > 27$ ). We therefore do not believe that there could be a visible supernova component in our first IR images.

### 2.4. Photometry and Light Curve

We calibrated each of our ground based nIR fields by use of secondary standards within the field of view of all telescopes. These stars are shown in Table 3. We performed aperture photometry on the standard stars and the afterglow candidate with the aperture being set

TABLE 1  
GROUND BASED OPTICAL AND NIR PHOTOMETRY OF THE AFTERGLOW OF GRB 030115

$\Delta t$ (days)	Inst./Filter	seeing (")	mag	$F_\nu$ Jy	$F_\nu$ (Host Subtracted)
0.11	Asiago/1.82m/R	2.5	$21.8 \pm 0.3$	$5.5 \times 10^{-6}$	$5.3 \times 10^{-6}$
0.21	KPNO2.1m/J	1.2	$19.19 \pm 0.11$	$3.31 \times 10^{-5}$	$3.20 \times 10^{-5}$
0.21	KPNO2.1m/H	1.2	$17.82 \pm 0.09$	$7.52 \times 10^{-5}$	$7.19 \times 10^{-5}$
0.21	KPNO2.1m/K	1.2	$16.84 \pm 0.05$	$1.19 \times 10^{-4}$	$1.14 \times 10^{-4}$
0.38	KPNO2.1m/J	1.3	$20.47 \pm 0.27$	$1.02 \times 10^{-5}$	$9.10 \times 10^{-6}$
0.38	KPNO2.1m/H	1.3	$18.37 \pm 0.16$	$4.53 \times 10^{-5}$	$4.19 \times 10^{-5}$
0.38	KPNO2.1m/K	1.3	$17.26 \pm 0.08$	$8.12 \times 10^{-5}$	$7.65 \times 10^{-5}$
1.11	WHT/H	1.3	$20.29 \pm 0.28$	$7.44 \times 10^{-6}$	$4.10 \times 10^{-6}$
1.22	NTT/J	0.7	$21.12 \pm 0.19$	$5.59 \times 10^{-6}$	$4.49 \times 10^{-6}$
1.23	NTT/H	0.7	$20.69 \pm 0.31$	$5.35 \times 10^{-6}$	$2.01 \times 10^{-6}$
1.25	NTT/K	0.7	$19.51 \pm 0.15$	$1.02 \times 10^{-5}$	$5.50 \times 10^{-6}$
1.14	VLT/FORS2/I	0.8	$23.8 \pm 0.20$	$8.00 \times 10^{-7}$	$4.02 \times 10^{-7}$
1.17	VLT/FORS2/R	0.8	$24.5 \pm 0.20$	$5.49 \times 10^{-7}$	$1.89 \times 10^{-7}$
1.21	VLT/FORS2/V	0.8	$25.1 \pm 0.30$	$3.88 \times 10^{-7}$	$1.68 \times 10^{-7}$
2.10	NOT/NOTCAM/K	1.0	$19.8 \pm 0.3$	$7.24 \times 10^{-6}$	$2.54 \times 10^{-6}$
2.12	VLT/ISAAC/K	0.7	$19.8 \pm 0.15$	$7.24 \times 10^{-6}$	$2.54 \times 10^{-6}$
2.20	VLT/FORS1/I	0.8	$24.0 \pm 0.3$	$7.24 \times 10^{-7}$	-
2.24	VLT/FORS1/R	0.8	$25.2 \pm 0.4$	$2.40 \times 10^{-7}$	-
<b>GCN data</b>	<i>Kato et al.</i>	2003a,b			
0.86	IRSF/J		$20.4 \pm 0.2$	$1.16 \times 10^{-5}$	$1.05 \times 10^{-5}$
0.86	IRSF/H		$19.9 \pm 0.3$	$3.90 \times 10^{-5}$	$3.56 \times 10^{-5}$
0.86	IRSF/K		$18.5 \pm 0.2$	$2.44 \times 10^{-5}$	$1.97 \times 10^{-5}$
1.96	IRSF/J		$21.5 \pm 0.5$	$4.2 \times 10^{-6}$	$3.10 \times 10^{-6}$
1.96	IRSF/H		$20.4 \pm 0.4$	$6.7 \times 10^{-6}$	$3.30 \times 10^{-6}$
1.96	IRSF/K		$19.1 \pm 0.1$	$1.4 \times 10^{-5}$	$9.30 \times 10^{-6}$

NOTE. — Table of observations of GRB 030115. Shown is the time since burst of each observation, the measured magnitude, flux and host subtracted flux. For the final two R and I band points, the flux levels are nominally above those measured for the host galaxy, but consistent within the measurement errors. All of the data points are corrected for foreground reddening  $E(B-V) = 0.024$ , assuming a MW extinction law.

TABLE 2  
OPTICAL AND NIR OBSERVATIONS OF THE GRB 030115 HOST GALAXY.

$\Delta t$ (days)	Inst./Filter	Exptime (s)	mag	$F_\nu$ (Jy)
26.466	<i>HST</i> /ACS/F606W	2000	$25.58 \pm 0.05$	$2.00 \times 10^{-7}$
26.406	<i>HST</i> /ACS/F814W	1600	$24.83 \pm 0.04$	$4.06 \times 10^{-7}$
26.268	<i>HST</i> /NICMOS/F160W	5120	$22.68 \pm 0.08$	$2.55 \times 10^{-6}$
126.193	<i>HST</i> /NICMOS/F110W	2558	$24.08 \pm 0.11$	$1.10 \times 10^{-6}$
127.672	<i>HST</i> /ACS/F814W	1920	$24.85 \pm 0.04$	$3.98 \times 10^{-7}$
151.975	<i>HST</i> /ACS/F435W	8800	$25.99 \pm 0.12$	$1.37 \times 10^{-7}$
156.071	<i>HST</i> /NICMOS/F222M	7678	$22.21 \pm 0.15$	$4.70 \times 10^{-6}$

NOTE. — Table of observations of the host galaxy GRB 030115 obtained with *HST*. The magnitudes have been calculated via SExtractor and are given as AB-magnitudes. They have been corrected for foreground extinction assuming  $E(B-V) = 0.024$ , and a MW extinction law. The magnitudes reported are those measured in an aperture determined by a SExtractor detection on the F160W image, then applied to other images which have been matched to this.

to twice the Full Width Half Maximum (FWHM) of the image. The RMS scatter observed in the magnitudes of the standard stars in each of the observations (from that expected and tabulated in Table 3) is less than 0.06 magnitudes.

The lightcurve of GRB 030115 in J, H and K is shown in Figure 2. Fitting the three bands simultaneously yields a power-law decay slope of  $\alpha = 1.26 \pm 0.06$ . However a single power-law is a relatively poor fit to the data, largely due to the second epoch J-band observation, which falls significantly below the expectation of the power-law at this time.

Extrapolating our R-band observations ( $R=21.7$  at

0.11 days) to the time of the first IR epoch (assuming  $t^{-1.26}$  as the decay slope) yields  $R=22.6$ , which results in an R-K colour of 5.7, making GRB 030115 one of the most reddened afterglows observed to date. However it should be noted that this extrapolation assumes that the afterglow behaviour is predictable over this time, the possible unusual behaviour of the J-band lightcurve and the frequent presence of bumps in the afterglow light curves of many GRBs mean that this value should be used with caution.

### 3. THE HOST GALAXY – PHOTOMETRIC REDSHIFT

The host galaxy of GRB 030115 (Fig. 4) shows an irregular morphology. The host may be involved in a

TABLE 3  
SECONDARY STARS USED FOR PHOTOMETRIC CALIBRATION IN THE  
GRB 030115 FIELD

RA(°)	Dec°	J	H	K
169.65241	15.06268	16.13 ± 0.02	15.63 ± 0.03	15.44 ± 0.10
169.64557	15.05777	15.84 ± 0.03	15.45 ± 0.01	15.36 ± 0.06
169.65432	15.04912	14.79 ± 0.02	14.15 ± 0.02	13.98 ± 0.02
169.61094	15.04204	15.93 ± 0.05	15.44 ± 0.04	15.08 ± 0.06
169.62917	15.03929	15.61 ± 0.05	15.17 ± 0.02	15.13 ± 0.06

merger with a companion galaxy offset approximately  $1''$  northeast of the host. The F435W image (the shortest wavelength used in this study) also shows evidence for an edge-on disk through the host galaxy. Our precise ISAAC astrometry allows us to position the afterglow at the southern end of this putative disk, with a positional accuracy of  $0''.05$  ( $1\sigma$ ). The host was observed with a complete filter set (B(V-R)IJHK) using both ACS and NICMOS. The results of photometry are shown in Table 1. The host has a very red R-K color (5.35), far redder than any other GRB host observed to-date. This color is dominated by a break between the J and H bands of 1.4 magnitudes (AB). It is possible that this represents the Balmer ( $4000 \text{ \AA}$ ) break, which could indicate the presence of an underlying older stellar population, however it is not possible to distinguish unambiguously between an strong break as might be expected from an older population and a very steep slope which could be indicative of a younger, but obscured system.

Knowledge of the redshift of GRB 030115 is essential to our understanding of the afterglow, and hence to the issue of “dark” bursts. Despite attempts from the ground to obtain spectroscopy of the host galaxy, the results were inconclusive. We have therefore sought to determine a photometric redshift from our B(V-R)IJHK photometry. In addition we have also determined photometric redshifts for other galaxies which fall within the field of view of our ACS and NICMOS images (the complete region has an area of  $0.51 \text{ arcmin}^2$ ) for a complete set of filters.

We have applied two independent codes. The first is the template fitting method of HYPERZ<sup>22</sup>; the second is the Bayesian method of Benítez (2000)<sup>23</sup>. They are outlined below but for more detail the reader is referred to Benítez (2000) (BPZ) and Bolzonella, Miralles & Pello (2000) (HYPERZ).

HYPERZ is a template fitting photometric redshift code. It provides a maximum likelihood redshift by performing  $\chi^2$  fitting of the available photometry with a variety of spectral templates: Starburst (Stb), Elliptical (E), Lenticular (S0), Irregular (Im) and a set of spiral templates of type Sa through Sd. In addition to the photometric redshift and extinction measures it is also possible to obtain an estimate of the age of the stellar population of the host galaxy. The impact of the assumed IMF when HYPERZ has been applied to host galaxies has been negligible (Gorosabel *et al.* 2003a,b; Christensen *et al.* 2004).

The Bayesian code (BPZ) works by making use of other available information information, rather than simply fitting templates. These priors take into account our

knowledge of the expected physical parameters of galaxies, such as their luminosity function, redshift distributions, and galaxy type fractions. Here we use a luminosity prior based on the observed luminosity function seen in the Hubble Deep Field. Therefore, in addition to the template fitting performed by HYPERZ, BPZ also determines the probability that a galaxy of that magnitude should be present at the redshift suggested by the linear fit. This can be effective at clipping “unreasonable” redshifts when template fitting alone finds two or more plausible fits.

Magnitudes for the photometric redshifts were determined by aligning and rebinning all of our ACS and NICMOS data to the same pixel scale, while preserving photometry (this was done via the IRAF tasks *geomap* and *geotran*). We then defined a detection mask on the F160W image and extracted magnitudes from the same physical region in other filters. We thus obtain a complete set of photometry to H=25(AB). The ACS images are significantly deeper than those obtained with NICMOS and therefore contain many galaxies which are not contained within our catalog. However in the absence of IR detections it is not possible to determine accurate photometric redshifts for these galaxies.

Based on these detection criteria we determine photometric redshifts of  $z = 2.50 \pm 0.20$  for HYPERZ and  $z = 2.70 \pm 0.25$  for BPZ. Individually the best fit redshift of the neighbour is found to be  $z = 2.65 \pm 0.30$  based on HYPERZ and  $z = 3.0 \pm 0.30$  based on BPZ. The colors of the neighbour galaxy are very blue (F814W-F160W (AB)= 1) and are typical of star forming galaxies containing little dust. The best fitting spectral type of the host galaxy is that of a S0 in HYPERZ and a Sb/c in BPZ. HYPERZ finds that the internal extinction within the host is moderately large  $A_V = 1.0$  and that its dominant stellar population is old; 2.6 Gyr. This age determination is largely due to the strength of the Balmer break which lies between the J and H bands at this redshift. If this age determination were correct it would imply a redshift of formation of  $z \sim 6.5$ . However, this age should be treated with caution since it has been noted that for Extreme Red Objects (EROs) the photometric shape alone cannot adequately distinguish between dusty, star forming galaxies and those which harbor an older population of stars (Moustakas *et al.* 2004).

#### 4. COMPARISON OF THE HOST PROPERTIES WITH OTHER GRB HOST GALAXIES

Given the very red color of both host and afterglow, it is obviously interesting to compare GRB 030115 with other host galaxies. Chary *et al.* (2002) and Le Floc’h *et al.* (2003) have imaged a sample of GRB host galaxies in the IR (K-band). Their measurements allow the deter-

<sup>22</sup> see <http://webast.ast.obs-mip.fr/hyperz/>

<sup>23</sup> see <http://adcam.pha.jhu.edu/~txitxo/bpzdoc.html>

mination of the global (R-K) color of the host galaxies and provide insight into the extinction and star formation rate. A important question relating to the nature of GRB hosts is whether these are typical of high- $z$  galaxies which are selected by other techniques (e.g., sub-mm surveys). These surveys indicate that the majority of high- $z$  star formation ( $z \sim 2$ ) is obscured with a significant fraction likely taking place in galaxies analogous to the lower redshift ULIRGs. The optical counterparts to these sub-mm bright galaxies are often very red, massive systems. By contrast, typical GRB host galaxies are mostly blue and sub-luminous, though the latter may be due to the steep luminosity function of star-forming galaxies (Fruchter *et al.* 1999; Hogg & Fruchter 1999; Fynbo *et al.* 2002; Le Floc'h *et al.* 2003). The R-K colors of GRB host galaxies are therefore apparently distinct from those of the typically red sub-mm emitting galaxies, and the few GRB host galaxies which do show sub-mm emission do not show any significant optical properties to distinguish them from other GRB hosts (Berger *et al.* 2003). In fact a sub-mm emitter, like the host of the dark GRB 000210, can show low extinction in the optical-nIR having colours typical of the bluest host galaxies (Gorobabel *et al.* 2003a). The host of GRB 030115 is, however, very red and lies at a redshift comparable to that of many sub-mm sources ( $z \sim 2.4$ ; Chapman *et al.* 2003). Although early sub-mm afterglow observations have only provided an upper limit to the  $850 \mu\text{m}$  flux (Hoge *et al.* 2003), the depth of these observations would not have been sufficient to detect any other GRB host to-date (Tanvir *et al.* 2004).

Figure 6 shows the R-K color of the host galaxies of GRBs versus their redshift. K-band data is taken from Le Floc'h *et al.* (2003) and Chary *et al.* (2002) (and references therein). The host galaxy of GRB 030115 lies significantly above the curve that represents the majority of the GRB host galaxies. Indeed its spectral type is best fit as an Sc; however it remains significantly underluminous in the optical (rest-frame UV) ( $R^* / 8$ ). In contrast it is apparently overluminous in the K-band ( $K^* \times 4$ ). It is possible that this is due to extinction within the disk of the host galaxy which we may view edge on. The majority of the optical light produced at the centre of the galaxy could then not escape through the dusty disk of the galaxy, resulting in its red color.

The absence of a single red sub-mm emitting galaxy from the list of GRB hosts is particularly puzzling given the widespread belief that most of the sub-mm emission from these objects is due to dust heating by massive stars (Le Floc'h *et al.* 2003; Fynbo *et al.* 2003). The presence of GRB 030115 within a very red host offers some evidence that a fraction of GRBs are extinguished and come from larger galaxies with red global colors; however the proportion of bursts which may lie within this class is very poorly constrained so far (see also Klose *et al.* 2000, 2003). Unfortunately, the faintness of the afterglow GRB 030115 in the optical, precluded high-resolution spectroscopic study of the ISM of the host.

#### 4.1. Host Galaxy Star Formation Rate and Extinction

At  $z \sim 2$  our broadband ACS images cover restframe wavelengths of approximately 1550, 2160 and 2900 Å for F435W, F606W and F814W, respectively. From this we can obtain a measure of the host galaxy extinction and

star formation rate.

Star formation measures based purely on the rest-frame UV luminosity are prone to significant errors due to the effects of dust scattering and absorption of UV light. Therefore unextinguished measurements provide only a lower limit on the star formation rate. Using the relation of Kennicutt (1998),

$$\text{SFR}(M_{\odot}\text{yr}^{-1}) = 1.4 \times 10^{-28} L_{\nu}(\text{erg s}^{-1} \text{Hz}^{-1} (1500\text{-}2800 \text{ \AA})), \quad (1)$$

we obtain an flux (uncorrected for dust extinction) of  $F_{\nu} = 2.13 \times 10^{-30} \text{ erg s}^{-1} \text{ cm}^{-2}$  which, using our choice of cosmology, implies a value of  $L_{\nu} = 4\pi d_l^2 F_{\nu} / (1+z) = 3.1 \times 10^{28} \text{ ergs s}^{-1} \text{ Hz}^{-1}$ . This gives a SFR of  $4.4 M_{\odot} \text{ yr}^{-1}$ , in the F606W passband.

Given the red colour of the observed afterglow we may expect that there is significant dust within the host galaxy and therefore substantial scattering and absorption of the restframe UV flux. This UV flux is then re-radiated in the far infrared. Meurer, Heckman & Calzetti (1999; hereafter M99) have calibrated this effect for local starburst galaxies and find a strong correlation between restframe ultraviolet spectral slope and flux at  $60 \mu\text{m}$ . Under the assumption that the relation found for local starbursts holds at higher redshifts (which may be expected, see section 2, M99) we can obtain a better measure of the star formation rate, and the extinction within the host galaxy. The relation given in M99 for extinction is

$$A_{1600} = 4.43 + 1.99\beta. \quad (2)$$

The relation for spectral slope for  $(F606W - F814W)_{AB}$  at redshift  $z$  is given by

$$\beta = 3.23(F606W - F814W)_{AB} - 5.22 + 2.66z - 0.545z^2. \quad (3)$$

This results in  $\beta = 0.44$ , corresponding to  $A_{1600} = 5.3$ . Correcting our results to this extinction implies a massive star formation rate of  $\sim 500 M_{\odot} \text{ yr}^{-1}$ .

While this result remains highly uncertain, taken together with the extreme red color of the host galaxy, makes GRB 030115 an excellent candidate for further sub-mm followup.

## 5. A POSSIBLE CLUSTER AT $Z \sim 2.5$

In addition to obtaining the photometric redshift for GRB 030115 we have also been able to extract photometric redshifts for other galaxies within the field. The ACS observations contain many more objects than the NICMOS data, due to its greater depth and field of view. However these observations do not provide sufficient color information to enable photometric redshifts to be accurately determined. Thus only objects detected in the F160W image with magnitudes brighter than  $F160W(AB) = 25.0$  are included in the photometric redshift fitting. Stellar objects are rejected based on their extent within the ACS images (which have a much smaller point spread function than the NICMOS observations). A total of 56 galaxies meet this requirement. The histogram of photometric redshifts determined by HYPERZ is shown in Fig 7. As can be seen there exists a strong peak in the redshift distribution at  $z = 2.5$ , the favoured photometric redshift for the host galaxy using these selection criteria. The RMS of galaxies at redshift  $2 < z < 3$  within this fit is  $\sim 0.12$ , indicating that there

may be an association (such as an edge-on sheet of galaxies) or possibly a cluster at this redshift. The galaxies which form this association are all galaxies with luminosity at, or somewhat large than  $L^*$  (in the H-band). We are therefore only seeing the brightest members, while the more numerous, fainter galaxies are not detected.

In order to quantify the potential significance of this association it is necessary to determine the level of overdensity which exists at this redshift. To achieve this we need to examine the distribution of redshifts seen in other deep surveys. Few ground based surveys reach the limits obtained here (although most cover a much wider area). The deep surveys which we chose to use here were the GOODS survey (Giavalisco *et al.* 2004), the Hubble Deep Field North (HDF-N) and South (HDF-S) and the Hubble Ultradeep Field (UDF). For the HDF-N and UDF there is deep NICMOS imaging in F110W and F160W, for the GOODS survey and the HDF-S the IR imaging comes from ground based observatories, mostly deep VLT/ISAAC imaging. The optical imaging in the HDF-N and HDF-S is by WFPC2 and in the case of GOODS and the UDF is with ACS. In order to confirm the accuracy of our photometric redshifts determined by HYPERZ we performed fits on each of the photometric catalogs and compared the accuracy with known spectroscopic redshifts. In order to compare our data with what can be obtained with similar quality data we restricted the catalogs from each of these surveys to  $F160W(AB) < 25$  or  $H(AB) < 25$  for ground based observation. We also used the same filter set as obtained for the host of GRB 030115 (in general this means that we did not include U-band observations).

A potential problem with the determination of photometric redshifts via the template fitting *only* is that at times the redshift is poorly constrained (due often to a very low  $\chi^2/dof$  ( $\ll 1$ )). This commonly leads to low redshift systems being placed in higher redshift bins. Bayesian techniques can solve this problem by eliminating systems which would be overly luminous at a given redshift. Using BPZ on both the HDF and the GRB 030115 field does reduce the number of objects lying in the  $2 < z < 3$  bin. However the Bayesian priors are based on observed luminosity functions of field galaxies whereas galaxies within clusters may be expected to be more luminous. In practice, using BPZ on the GRB 030115 resulted in 5 objects being removed to a lower redshift bin and a slight broadening of the measured peak. Nonetheless the apparent overdensity remains, favoring a cluster at the redshift of the GRB host galaxy. Also comparison of the photometric redshifts with the known spectroscopic redshifts in the HDF and the GOODS survey implies that with our choice of filters and limiting magnitudes  $< 10\%$  of low redshift galaxies are placed at  $z > 2$  by HYPERZ. Thus we conclude that at most  $\sim 20\%$  of the galaxies placed in the  $2 < z < 3$  bin are falsely located. Even if these are removed there remains a substantial overdensity in the expected number of galaxies at this redshift, and we conclude that this is most likely a true association, and possibly a cluster of which the host galaxy of GRB 030115 is a member.

Without spectroscopic redshifts for a number of members we cannot determine the nature of the structure which we see unambiguously; it is possible that it is a larger scale association with a broad velocity dispersion

which is not gravitationally bound. However should the depth of this overdensity be comparable to its observed width in our HST images, then the association would be a cluster comparable in richness to that of Coma (Somerville 2004).

Figure 8 shows the histogram of colours for all galaxies found to lie in the redshift range  $2 < z < 3$ . While a few can be seen to have red colors comparable to the GRB host galaxy, the majority of the objects have much bluer colors, consistent with their being star-forming galaxies at this redshift. The host itself is typical of what would be expected of a galaxy in the center of a cluster at its redshift: a red and luminous galaxy still forming stars but in the process of evolving into a modern day elliptical.

### 5.1. The number of density of EROs about GRB 030115

EROs are generally defined by a color cut at around  $R-K = 5$ , although various other more stringent cuts eg.,  $R-K > 5.35$ ,  $R-K > 6$ , are also used. The original definitions for EROs were based on the expected colors of primeval elliptical galaxies (Elston *et al.* 1988). In practice EROs consist both of old passive systems (Daddi *et al.* 2000) and dusty star forming galaxies.

Our deepest IR image, and thus that most suitable to the discovery of red objects is F160W (approximately H-band). Thus we chose equivalent colors of  $F814W-F160W > 1.85$  (AB), which is an effectively identical spectral slope to  $R-K=5$  in Vega magnitudes. In our region (approximately  $0.5 \text{ arcmin}^2$ ) we find a total of 5 galaxies meeting this criterion. Three of these lie within the  $z = 2.5$  overdensity with the other two having poor photometry (4 rather than 6 colors with non-detections at F110W and F222M) fitting better at  $z \sim 0.7$ , but also having acceptable fits ( $\chi^2/dof < 2$ ) at  $z = 2.5$ .

We have also searched a larger region surrounding GRB 030115 by using our ACS image in conjunction with the K-band image obtained with ISAAC. The GRB still contributes some flux in this image and therefore the photometry of the host galaxy is not reliable. We determine that there are  $\sim 10$  EROs within this  $3.2 \text{ arcmin}^2$  region to a limit of  $K < 23$  (AB). Comparing this with ERO number counts (e.g. Moustakas *et al.* 2004; Gilbank *et al.* 2003) we find that they are overdense by a factor  $\sim 2$ . In practice using the ‘‘average’’ number of EROs is somewhat misleading since EROs are often highly clustered. Figure 9 shows the color magnitude diagram for the GRB 030115 region.

## 6. THE ORIGIN OF THE OPTICAL FAINTNESS OF GRB 030115

### 6.1. Extinction

GRB 030115 exhibits an exceptionally red color ( $R - K \approx 6$ ) but was not at extreme redshift. This is very unusual for GRB afterglows which typically have spectra well described as  $\nu^{-1}$ , corresponding to  $R - K = 2.9$ . Furthermore the color of the GRB 030115 afterglow is not well defined by a single power-law, but has significant curvature in the spectral energy distribution occurring at shorter wavelengths. The reddening of the afterglow due to extinction within the Milky Way is probably small,  $E(B - V) = 0.024$  (Schlegel, Finkbeiner & Davies 1998), making extinction in the host galaxy the most likely explanation. In order to estimate the extinction along the

line of sight to GRB 030115 we fit the afterglow with an extinction model of the form  $F_\nu = \nu^\beta \times 10^{-0.4A_\nu}$ . We have attempted to obtain the extinction at a given frequency  $A_\nu$ , based on the fitting models given by Pei (1993), relevant for differing dust to gas ratios and metallicities which are reflected in the MW, LMC and SMC. These fits result in unphysical parameters for the afterglow spectrum (namely  $\beta > 0$ , and  $A_V = 4$ , with MW-like extinction), this is true at all redshifts.

The precision of the above measurement could be compromised by several effects. The first is that while the afterglow is bright (and hence the errors small) we only obtain a truly simultaneous SED in three colors (J,H,K) while the R-band data must be extrapolated over a factor 2 in time. The afterglow does not appear to exhibit a “pure” power-law behaviour and this this extrapolation introduces a larger uncertainty into the spectral energy distribution that simply the photometric uncertainty associated with the measurement. As such deviations from a single power-law decline may naturally explain the poor fit obtained for the extinction laws described above). Furthermore, at later times (i.e.  $>24$  hours) the errors in the individual photometric points are large, and also contain a host contribution which further reduce their accuracy.

A possible physical explanation is that of dust destruction local to the GRB. Under many schemes (e.g., Waxman & Draine 2000; Fruchter, Krolik & Rhoads 2001) dust can be destroyed by the prompt X-ray/EUV emission over a distance of several hundred parsecs about the burst site. This dust destruction removes the small grain sizes, leaving the larger ones unaffected and will change the extinction law to one dominated by larger grains (e.g., Maiolino *et al.* 2000). The true extinction along our sight line to the GRB is then the composite of the dust local to the GRB environment and that at larger distances in the host galaxy (which in this case shows evidence of being dusty). The true extinction law may possibly be very different from those which describe sources in the local Universe and this is the likely reason for the poor fit of these laws to our data. A final possibility is that the afterglow spectrum has some intrinsic curvature, most likely due to the cooling break being in the IR-band at the time of the observation; however the apparent color changes seen in the second epoch are not easily explained as the cooling break, especially since later data are not consistent with this steepened slope.

### 6.2. A dark burst caught?

It is instructive to compare the colors of the host galaxy of GRB 030115 with those of the host galaxies of other GRBs, which typically exhibit blue colors (e.g., Fruchter *et al.* 1999). Fig. 10 (left) shows the R-magnitude of a selection of GRBs plotted against the R–K color of their host galaxies. While this plot is limited by small number statistics, it can clearly be seen that of the GRBs seen in the R-band at  $\Delta t=24$  hours, GRB 030115 is the faintest, and also lies in the most reddened host galaxy. The best fit line is shown, however much power is provided to this fit by GRB 030115 and it is therefore not possible to conclusively demonstrate a real trend whereby dark (faint) GRBs lie in reddened host galaxies.

Fig. 10 (right) shows the colors of GRB afterglows, plotted against the colors of their host galaxies. We

have plotted the effective power-law index  $\beta$  across the broadest range of wavelengths available for an individual burst. This plot shows little evidence for any correlation between host color and afterglow color, however the extreme nature of GRB 030115 can be clearly seen since both afterglow and host galaxy are very red.

The magnitude of GRB 030115 at  $\Delta t=24$  hours is the faintest GRB ever detected in the optical at this epoch. The magnitude is deeper than the limits placed on many other “dark” GRBs (see Fig. 11). This implies that GRB 030115 lies in a region of parameter space which would have been consistent with a dark GRB.

## 7. CONCLUSIONS

We have reported the discovery of the afterglow of GRB 030115. Originating from a (photometrically determined) redshift of  $\sim 2.5$ , the afterglow was the faintest seen in the R-band after 24 hours. The decay rate was faster than the mean of most GRBs with an average decay rate over the first 24 hours of  $\alpha \sim 1.5$ . The faintness of the afterglow in the optical is therefore likely a function of both this rapid decline and its extremely red spectrum.

Comparison of both the afterglow and host galaxy with those observed for other GRBs implies that the latter is the most reddened of any GRB host galaxy for which an afterglow has been seen. This is in contrast to some previous cases where red afterglows have been observed to lie in blue galaxies (e.g. GRB 000418, Klose *et al.* 2001; Gorosabel *et al.* 2003). However none of these afterglows is as extreme as that of GRB 030115, which has a flux density below the upper limits set for the large majority of dark GRBs at similar epochs. It may therefore be that some of the dark GRBs so far observed evolved in similar ways to GRB 030115 and were simply missed due to the lack of early IR observations. IR-robotic observations (e.g., REM, Liverpool Telescope) may be very successful at locating such afterglows in the future and will therefore provide valuable statistics on the number of GRBs occurring in obscured galaxies. In turn these GRB hosts offer a useful tool in characterising the nature of embedded star formation. Indeed moderate resolution spectroscopy of these sources at early times may be one of the best means of providing a detailed study of the environments of such galaxies, which are too optically faint for normal absorption line studies.

GRB 030115 also lies in a potentially significant overdensity of galaxies at  $z \sim 2.5$ . This association consists of a high ERO density, consisting of either dust enshrouded star formation or old, passive systems as well as bluer systems with active unobscured star formation. This association represents one of the richest associations found at  $z > 2$ .

However, further observations are necessary to confirm the existence of this cluster. Thus far, we have found low-redshift GRBs in field galaxies, however, we expect that as we study GRBs at higher redshifts, we should begin to find them, like GRB 030115, in clusters or in far richer regions of the Universe directly associated with star formation.

## ACKNOWLEDGEMENTS

We thank the referee for an very constructive report which greatly enhanced this paper. Support for Pro-

posal number GO 9405 was provided by NASA through a grant from the Space Telescope Science Institute, which is operated by the Association of Universities for Research in Astronomy. Incorporated under NASA contract NAS5-26555. This work was conducted in part via collaboration within the the Research and Training Network “Gamma-Ray Bursts: An Enigma and a Tool”, funded by the European Union under contract number HPRN-CT-2002-00294. AJL acknowledges the receipt

of a PPARC studentship. JMCC acknowledges the receipt of a FPI doctoral fellowship from Spain’s Ministerio de Ciencia y Tecnología. This work was supported by the Danish Natural Science Research Council (SNF) and partly based on observations made with the Nordic Optical Telescope, operated on the island of La Palma jointly by Denmark, Finland, Iceland, Norway, and Sweden, in the Spanish Observatorio del Roque de los Muchachos of the Instituto de Astrofísica de Canarias.

## REFERENCES

- Alard, C., Lupton, R., 2000, *ApJ*, 503, 325  
 Anderson, M.I., *et al.* 2000, *A&A* 364, L54  
 Barnard, V. E. *et al.* 2003, *MNRAS* 338,1  
 Benítez, N. 2000, *ApJ*, 536, 571  
 Berger, E., *et al.* 2003, *Nature*, 426, 154  
 Berger, E., *et al.* 2002, *ApJ*, 581, 981  
 Berger, E., Cowie, L.L., Kulkarni, S.R., Frail, D.A., Aussell, H., Barger, A.J., 2003, *ApJ*, 588,99  
 Berger, E., Frail, D.A., 2003, *GCN circ.* 1817  
 Bersier, D., *et al.*, 2003, *ApJ*, 584, 43  
 Bertoldi, F., Frail, D. A., Berger, E., Menten, K. M., & Kulkarni, S. 2003, *GCN circ.* 1835  
 Blake, C., Lamb, D. Q., Barentine, J., Dembicky, J., McCall, B., York, D. G., & McMillan, R. 2003, *GRB Circular Network*, 1808, 1  
 Bloom, J. S., Frail, D. A., & Kulkarni, S. R. 2003, *ApJ*, 594, 674  
 Bolzonella, M., Miralles, J.-M., & Pelló, R. 2000, *A&A*, 363, 476  
 Calzetti, D., Armus, L., Bohlin, R. C., Kinney, A. L., Koornneef, J., & Storchi-Bergmann, T. 2000, *ApJ*, 533, 682  
 Castro, S., *et al.* 2003, *ApJ*, 586, 128  
 Castro-Tirado, A. J., *et al.* 1999, *Science*, 283, 2069  
 Castro-Tirado, A. J., *et al.* 2001, *A&A*, 370, 398  
 Castro-Tirado A.J., Gorosabel, J., Casabova, V., 2003, *GCN circ.* 1807  
 Cavanagh, B., Hirst, P., Jenness, T., Economou, F., Currie, M. J., Todd, S., & Ryder, S. D. 2003, *ASP Conf. Ser.* 295: *Astronomical Data Analysis Software and Systems XII*, 12, 237  
 Chapman, S. C., Blain, A. W., Ivison, R. J., & Smail, I. R. 2003, *Nature*, 422, 695  
 Chary, R., Becklin, E.E., Armus, L., 2003, *ApJ*, 566, 229  
 Christensen, L., Hjorth, J., Gorosabel, J., Vreeswijk, P., Fruchter, A., Sahu, K., & Petro, L. 2004, *A&A*, 413, 121  
 Covino, S., *et al.* 2003, *A&A*, 404, L5  
 Crew, G. B., *et al.* 2003, *ApJ*, 599, 387  
 Daddi, E., Cimatti, A., Pozzetti, L., Hoekstra, H., Röttgering, H. J. A., Renzini, A., Zamorani, G., & Mannucci, F. 2000, *A&A*, 361, 535  
 Diercks, A., *et al.*, 1998, *ApJ*, 503, L105  
 Djorgovski, S. G., Frail, D. A., Kulkarni, S. R., Bloom, J. S., Odewahn, S. C., & Diercks, A. 2001, *ApJ*, 562, 654  
 Dullighan, A., Ricker, G., Butler, N., & Vanderspek, R. 2004, *AIP Conf. Proc.* 727: *Gamma-Ray Bursts: 30 Years of Discovery*, 727, 467  
 Elston, R., Rieke, G. H., & Rieke, M. J. 1988, *ApJ*, 331, L77  
 Flaccomio, E., Garnavich, P., & Stanek, K. 2003, *GCN circ.* 1806  
 Fox, D. W., *et al.* 2003, *Nature*, 422, 284  
 Fox, D. W. 2002, *GCN circ.* 1564  
 Frail, D.A., Berger, E., 2003, *GCN circ.* 1827  
 Frail, D. A., Kulkarni, S. R., Berger, E., & Wieringa, M. H. 2003, *AJ*, 125, 2299  
 Fruchter, A. S. & Hook, R. N. 2002, *PASP*, 114, 144  
 Fruchter, A., Krolik, J. H., & Rhoads, J. E. 2001, *ApJ*, 563, 597  
 Fruchter, A. S., *et al.* 1999, *ApJ*, 519, L13  
 Fynbo, J. U., *et al.* 2001, *A&A*, 369, 373  
 Fynbo, J. P. U., *et al.* 2002, *A&A*, 388, 425  
 Fynbo, J. P. U., *et al.* 2003, *A&A*, 406, L63  
 Galama, T. J., *et al.* 1999, *A&AS*, 138, 451  
 Galama T., *et al.* 2000, *ApJ*, 536, 185  
 Galama, T. J., *et al.* 2000, *ApJ*, 541, L45  
 Galama, T.J., *et al.* 2003, *A&A*, 406, L63  
 Gladders, M., Hall, P., *GCN circ.* 1495  
 Gorosabel, J., *et al.* 2002, *A&A*, 384, 11  
 Gorosabel, J. *et al.* 2002, *GCN circ.* 1651  
 Gorosabel, J., *et al.* *A&A*, 437, 411  
 Gorosabel, J., *et al.* 2003a, *A&A*, 409, 123  
 Gorosabel, J., *et al.* 2003b, *A&A*, 400, 127  
 Greiner, J., *et al.* 2003, *ApJ*, 599, 1223  
 Groot, P. J., *et al.* 1998, *ApJ*, 493, L27  
 Harrison, F. A., *et al.* 2001, *ApJ*, 559, 123  
 Hjorth J., *et al.* 2002, *ApJ*, 576, 113  
 Hjorth, J., *et al.* 2003, *Nature*, 423, 847  
 Hoge, J. C., Stevens, J. A., Moriarty-Schieven, G., & Tilanus, R. P. J. 2003, *GCN circ.* 1832  
 Hogg, D. W. & Fruchter, A. S. 1999, *ApJ*, 520, 54  
 Holland, S., Björnsson, G., Hjorth, J., & Thomsen, B. 2000, *A&A*, 364, 467  
 Holland, S.T., *et al.* 2003, *AJ*, 125, 2291  
 Kato D., *et al.* 2003, *GCN circ.* 1830  
 Kawai N., *et al.* 2003, *GCN circ.* 1816  
 Kennicutt, R. C. 1998, *ARA&A*, 36, 189  
 Klose, S., *et al.* 2000, *ApJ*, 545, 271  
 Klose, S., *et al.* 2003, *ApJ*, 592, 1025  
 Lamb, D., *et al.* 2003, *astro-ph/0310414*  
 Lazzati, D., Covino, S., & Ghisellini, G. 2002, *MNRAS*, 330, 583  
 Le Floch, E., *et al.* 2003, *A&A*, 400, 499  
 Levan, A.J., Merrill, M., Rol, E., Dell’Antonio, I., Rhoads, J., Fruchter, A.S., 2003, *GCN circ.* 1818  
 Maiolino, R., Marconi, A., Salvati, M., Risaliti, G., Severgnini, P., Oliva, E., La Franca, F., & Vanzani, L. 2001, *A&A*, 365, 28  
 Masetti N., Palazzi, E., Pian, E., 2003a, *GCN circ.* 1811  
 Masetti N., *et al.* 2003b, *A&A*, 404, 465  
 Masetti N., Palazzi, E., Pian, E., 2003b, *GCN circ.* 1823  
 Matheson, T., *et al.* 2003, *ApJ*, 582, 5  
 Mészáros, P. 2002, *ARA&A*, 40, 137  
 Meurer, G. R., Heckman, T. M., & Calzetti, D. 1999, *ApJ*, 521, 64  
 Miller, G. E. & Scalzo, J. M. 1979, *ApJS*, 41, 513  
 Moustakas, L. A., *et al.* 2004, *ApJ*, 600, L131  
 Panaitescu, A. & Kumar, P., 2001, *ApJ*, 554, 667  
 Pei, Y. C. 1992, *ApJ*, 395, 130  
 Priddey, R. S., Tanvir, N. R., Levan, A. J., Fruchter, A. S., Kouveliotou, C., Smith, I. A., & Wijers, R. A. M. J. 2006, *MNRAS*, 369, 1189  
 Reichart, D.E., *et al.* 1999, *ApJ*, 517, 692  
 Rhoads, J. E. & Fruchter, A. S. 2001, *ApJ*, 546, 117  
 Rhoads, J. E. 2001, *ApJ*, 557, 943  
 Rol, E. & Wijers, R. 2003, *GCN circ.* 1864  
 Sahu, K. *et al.* 2000 *ApJ*, 540, 74  
 Sari, R., Piran, T. & Narayan, R., 1998, *ApJ*, 497, L17  
 Savaglio, S., Fall, S. M., & Fiore, F. 2003, *ApJ*, 585, 638  
 Schlegel, D. J., Finkbeiner, D. P., & Davis, M. 1998, *ApJ*, 500, 525  
 Smail, I., Ivison, R. J., Kneib, J.-P., Cowie, L. L., Blain, A. W., Barger, A. J., Owen, F. N., & Morrison, G. 1999, *MNRAS*, 308, 1061  
 Smail, I., Ivison, R. J., Blain, A. W., & Kneib, J.-P. 2002, *MNRAS*, 331, 495  
 Somerville, R. S. 2004, *ArXiv Astrophysics e-prints*, *astro-ph/0401570*  
 Stanek, K. Z., Garnavich, P. M., Kaluzny, J., Pych, W., & Thompson, I. 1999, *ApJ*, 522, L39  
 Tanvir, N. R. *et al.* 2004, *MNRAS*, 352, 1073  
 Taylor, G. B., Frail, D. A., Kulkarni, S. R., Shepherd, D. S., Feroci, M., & Frontera, F. 1998, *ApJ*, 502, L115  
 Taylor, G. B., Bloom, J. S., Frail, D. A., Kulkarni, S. R., Djorgovski, S. G., & Jacoby, B. A. 2000, *ApJ*, 537, L17  
 Vrba F., Luginbuhl, C., Henden, A., 2003, *GCN circ.* 1822  
 Vreeswijk, P.M., *et al.* 1999, *ApJ*, 523, 171  
 Wang, X. & Loeb, A. 2000, *ApJ*, 535, 788  
 Waxman, E. & Draine, B. T. 2000, *ApJ*, 537, 796

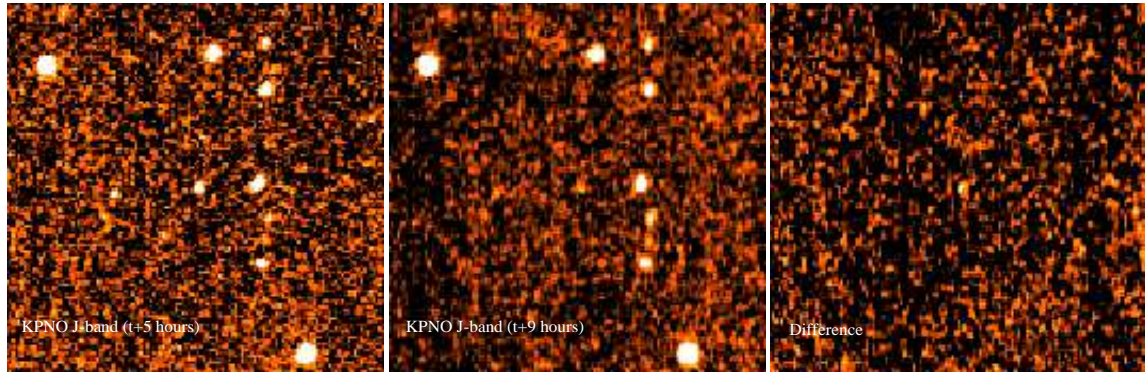


FIG. 1.— The discovery of GRB 030115: The left panel shows an image obtained with KPNO 2.1 + SQUIID in the J band 5 hours after burst. The central shows an image obtained in the same configuration after 9 hours, and the right hand panel shows the results of a PSF matched image subtraction, the afterglow is at the centre of the image.

Yost *et al.* 2002, ApJ, 577, 155

Zeh, A., Klose, S., & Hartmann, D. H. 2004, ApJ, 609, 952

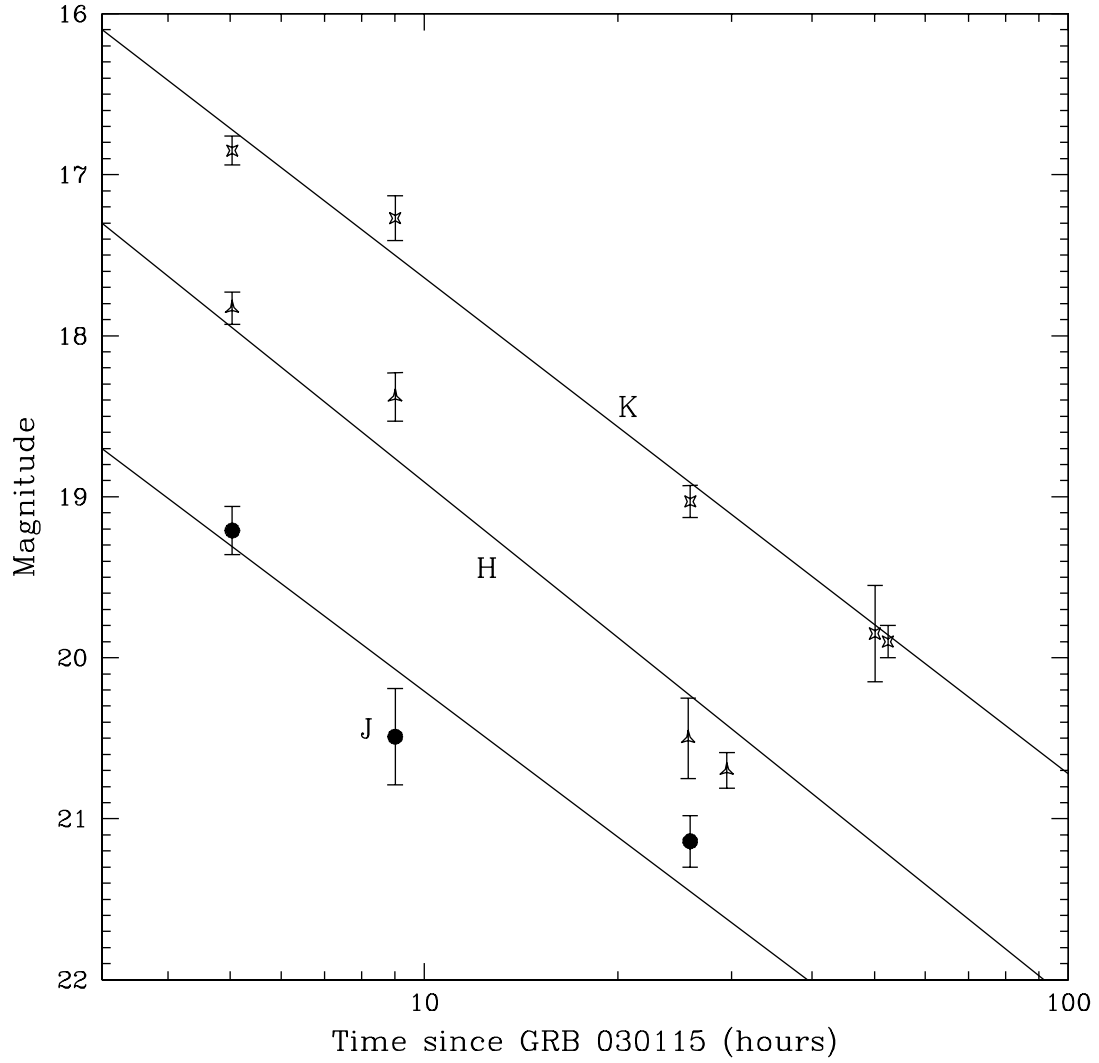


FIG. 2.— The nIR light curve of GRB 030115 in J, H and K. A broken power-law fit is shown and is a good fit to the H and K band light curves. The J band lightcurve does not fit this model due to the  $\Delta t=9$  hour point.

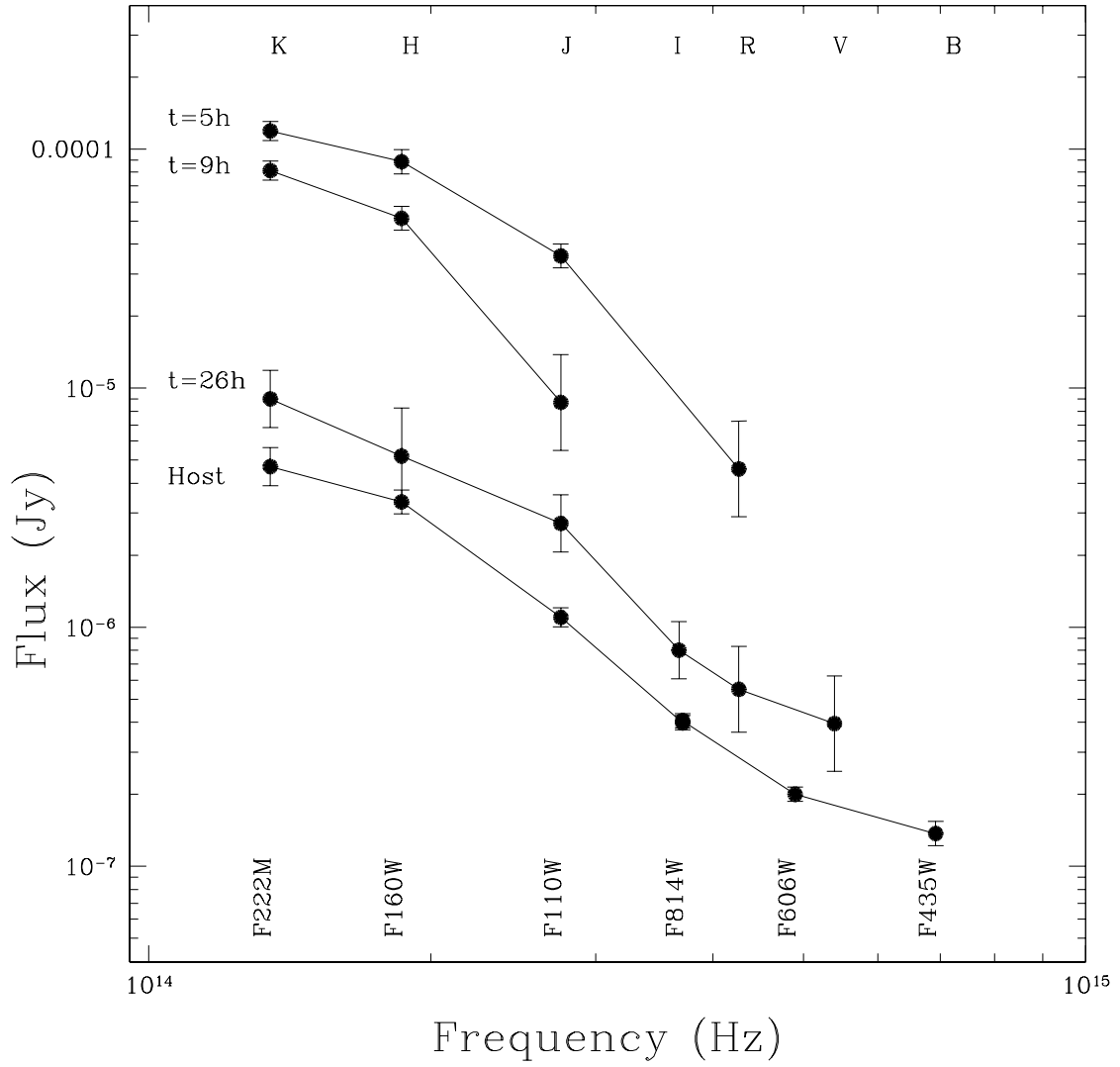


FIG. 3.— The evolution of the spectral energy distribution (SED) of GRB 030115 with time, marginal evidence of color evolution can be seen between 5 and 9 hours however the reality of this cannot be assessed since it is apparent in only one data point. The fluxes shown have been corrected for the effects of galactic extinction.

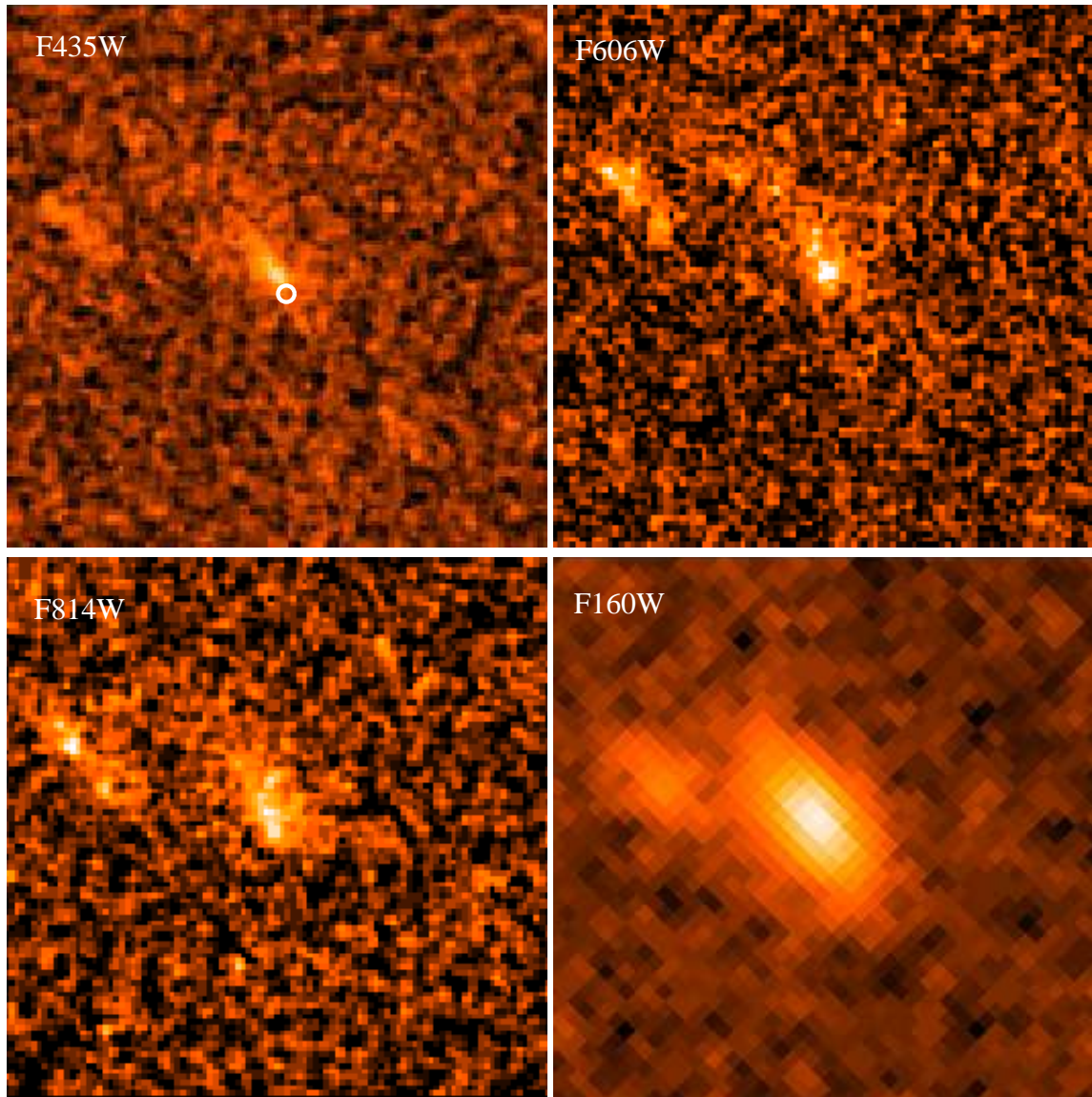


FIG. 4.— The host galaxy of GRB 030115 as seen by *HST* using ACS and NICMOS. The position of the afterglow is marked as a white circle of the F435W image (top left), with the radius of the circle marking the  $1\sigma$  confidence level. The possibly interacting galaxy can be seen to the upper left (northeast) in each of the images). The field of view of the images is  $\sim 3''$

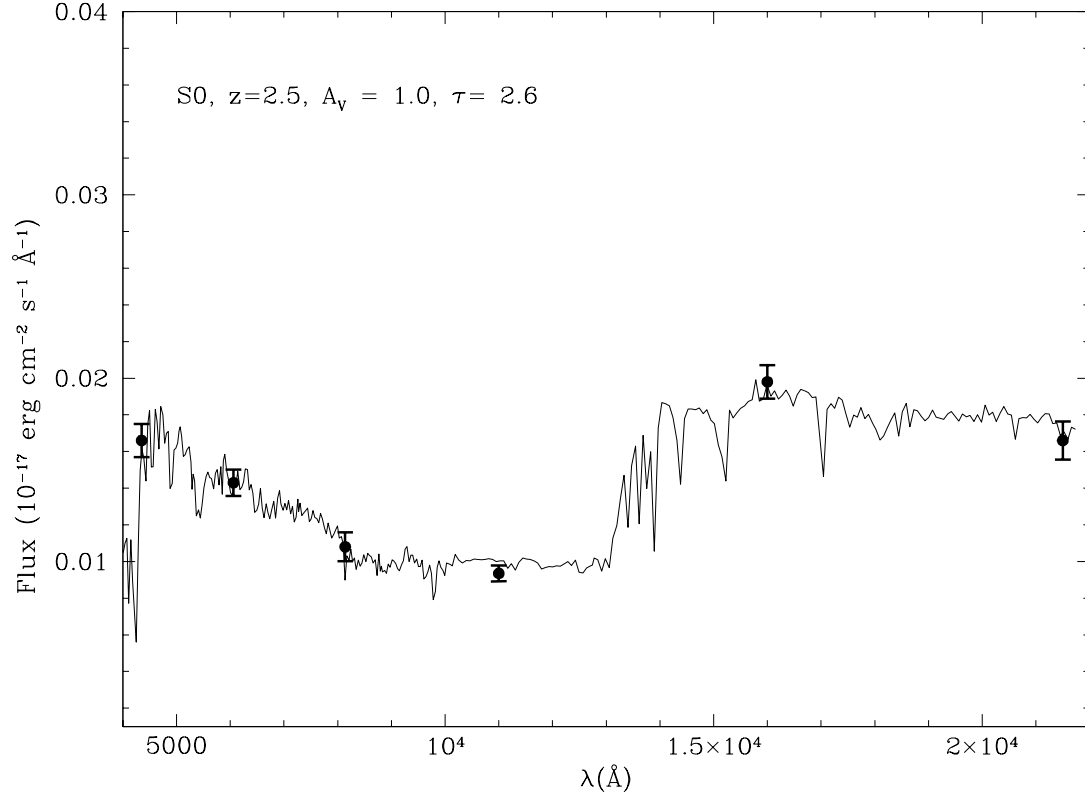


FIG. 5.— The best fitting spectral energy distribution for the host galaxy of GRB 030115, shown as an Sc-galaxy at  $z = 2.16$ , as found by HYPERZ, overplotted are the photometric points from *HST*.

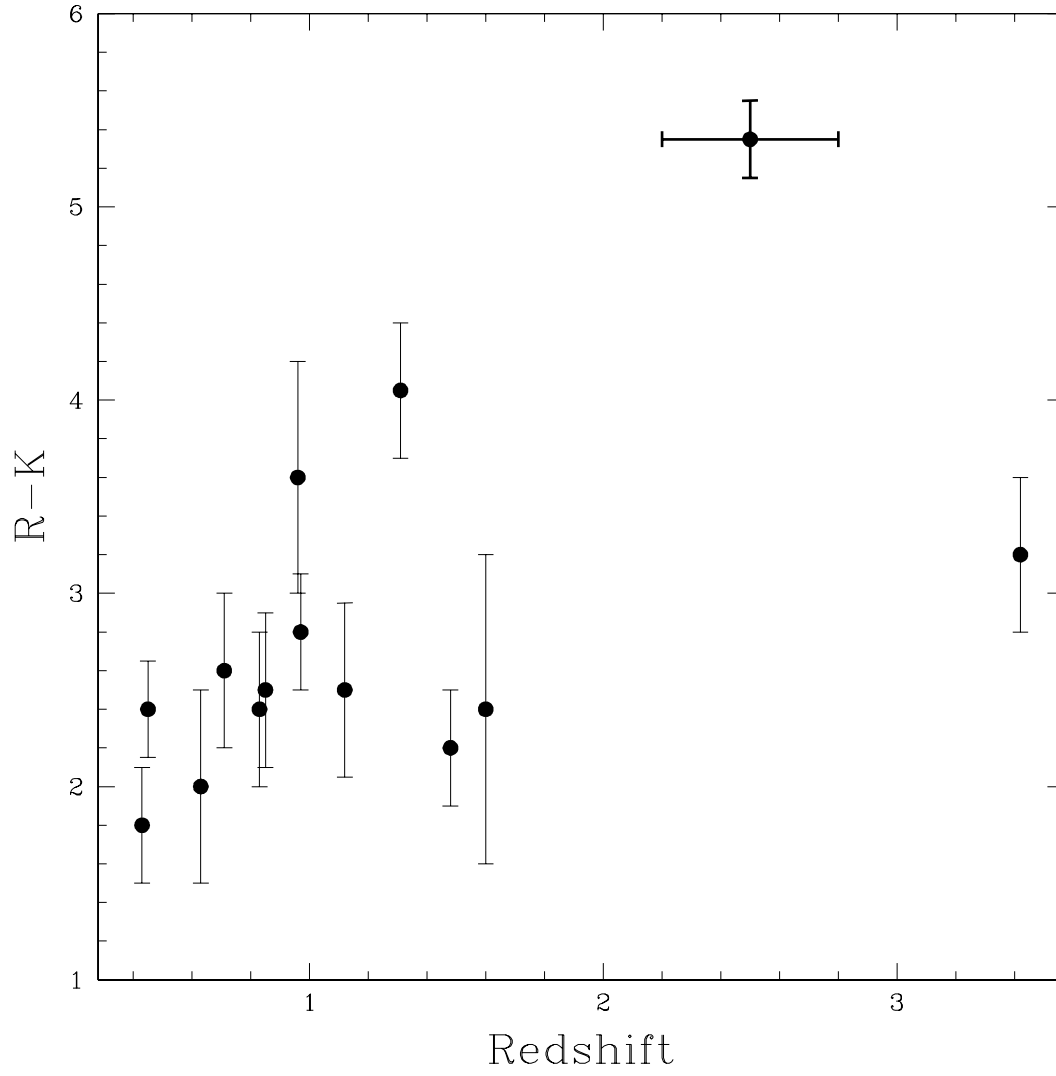


FIG. 6.— The (R-K) colours of GRB host galaxies as a function of redshift (data taken from Le Floc'h *et al.* 2003), the host of GRB 030115 is shown in bold (with the errorbar in  $z$ ) it can be seen to lie significantly above the typical R-K colors of GRB hosts.

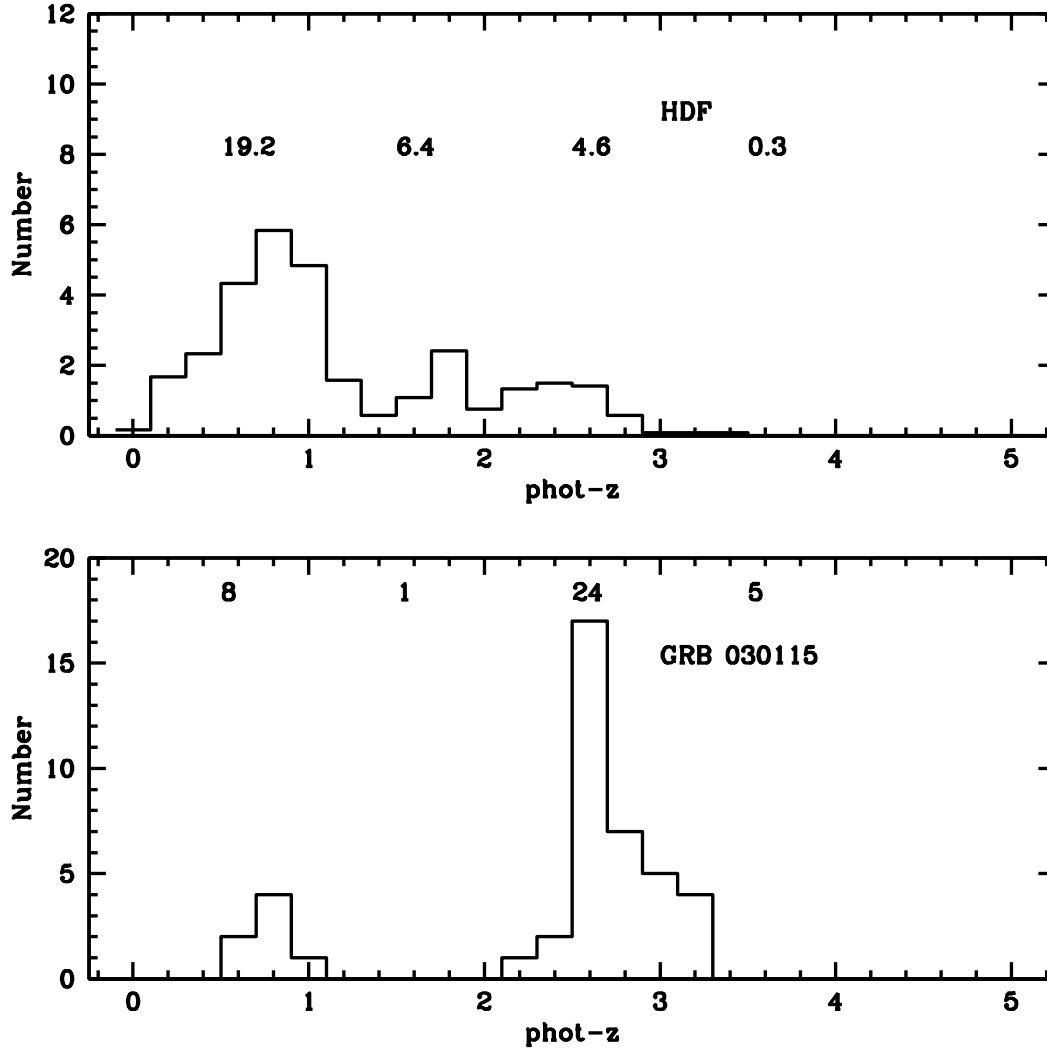


FIG. 7.— Histogram of photometric redshifts for the HDF (top) and the GRB 030115 field (bottom). The HDF photometric redshifts were determined from a catalog with  $F_{160W}(AB) < 25$  and with the omission of the U-band data. They have been normalised to represent the expected numbers in the GRB 030115 field surveyed. The numbers above each histogram represent the number of objects found to lie in the redshift bins  $0 < z < 1$ ,  $1 < z < 2$ ,  $2 < z < 3$  and  $3 < z < \infty$  by HYPERZ. The possible biases within this determination are discussed in Section 5.

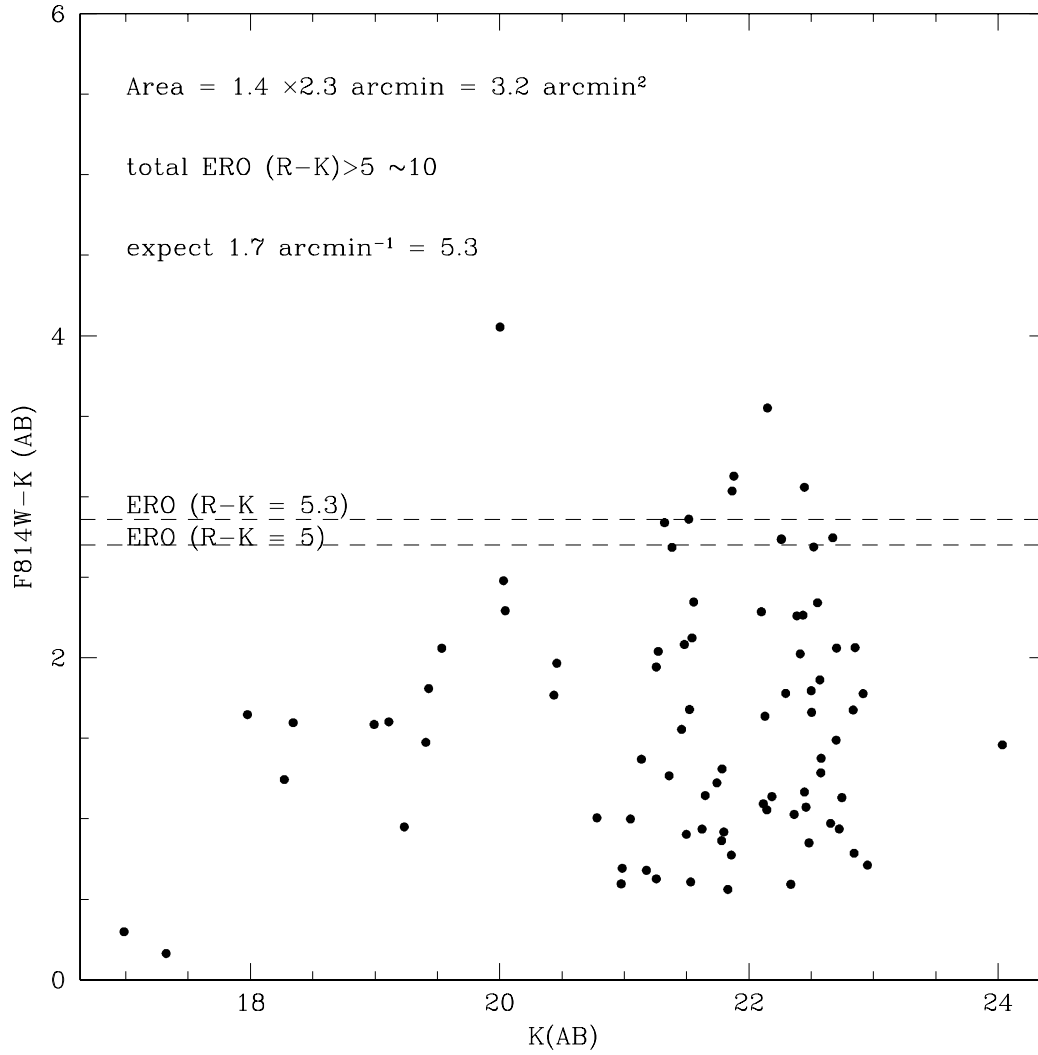


FIG. 8.— The color magnitude plot for the GRB 030115 field, compiled with a combination of ACS and ISAAC data. The color cuts which correspond to spectral slopes appropriate for  $R-K=5$  and  $R-K=5.35$  are shown. Approximately 10 galaxies in this field are EROs to a limiting magnitude of  $K(\text{AB}) = 23$ , there are also a number of other galaxies with very red (but not extremely red) colors. This is a factor of  $\sim 2$  overdense with respect to EROs studied within the *GOODs* field.

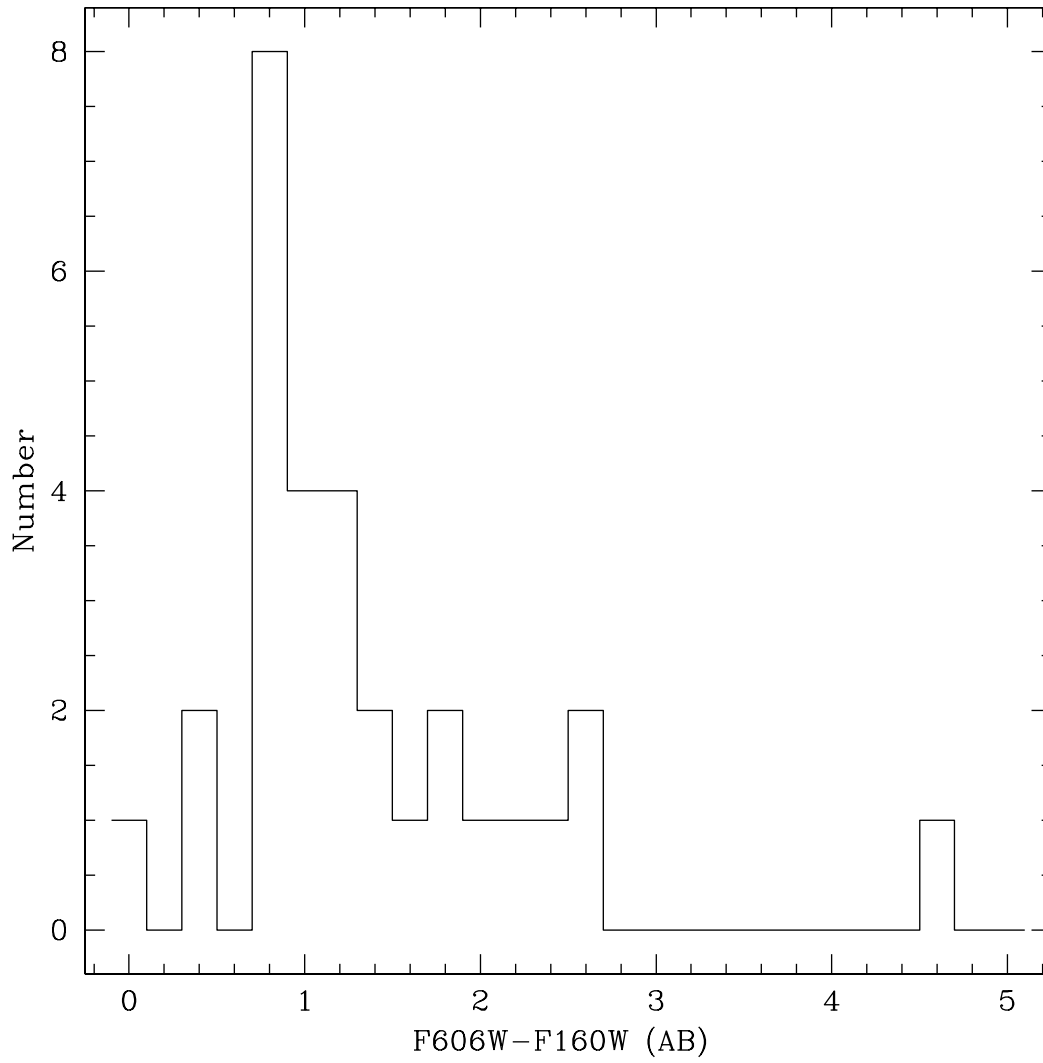


FIG. 9.— Histogram of the colors of possible cluster members for GRB 030115. Although some are very red objects, indicating an older stellar population many exhibit blue colors ( $F606W-F160W(AB) = 1$ ), which are typical of star forming systems.

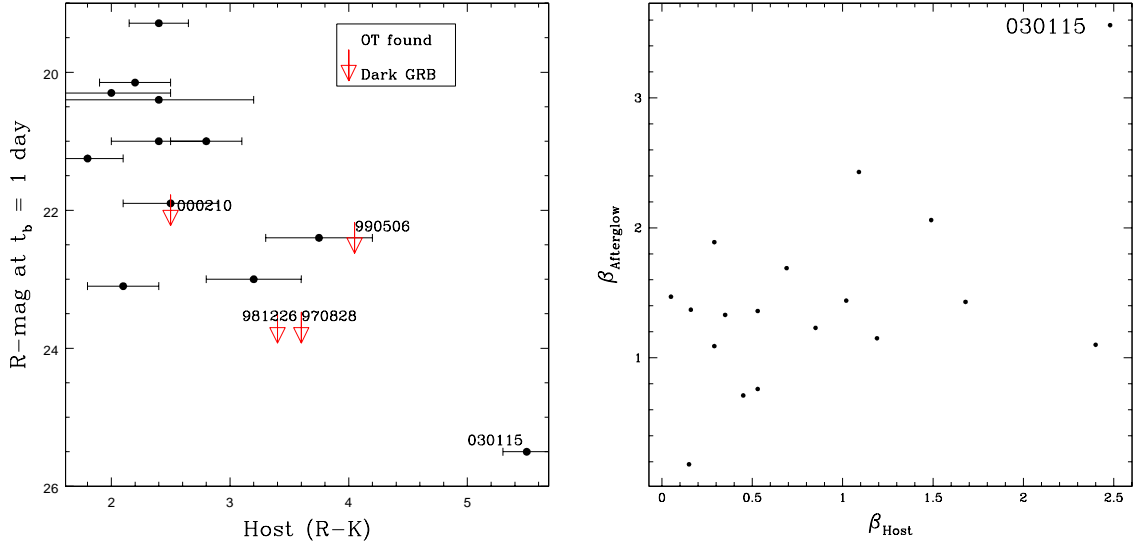


FIG. 10.— The extreme colors of GRB 030115 and its host galaxy: *left*: The broadband colours of GRB host galaxies ( $R-K$ ) versus the  $R$ -magnitude of their afterglows at  $\Delta t=1$  day. In cases where observations at 1 day are not available the magnitude is calculated from an extrapolation of a point near one day, based on the published decay slope for each burst. The red arrows indicate the limits placed on the dark GRBs. The assumed decay law (for extrapolating the limits to  $\Delta t=1$  day is  $\alpha = 1$ ). The solid line indicates the least squares fit to the data. Only those bursts with solid detections have been used in the fit. The dark bursts are plotted for comparison. *right*: The colours of GRB afterglows and their host galaxies, plotted against one another. The determination of  $\beta$  is done on the widest wavelength range available for a given afterglow or host galaxy. In each case the range of wavelengths used for the determination of  $\beta$  is the largest available. In order to ascertain the colours the magnitudes have been normalised to a common epoch using the published values of  $\alpha_1$ ,  $\alpha_2$  and  $\Delta t$  (the pre and post-break decay slopes, and the time of the break, under the assumption that it is the jet break) and assuming an achromatic evolution. For low redshift afterglows colour information is taken from the early afterglow, where supernovae contamination should not affect the observed colour. The majority of host colors have been obtained from Le Floch *et al.* 2003; and Chary *et al.* 2002. The afterglow colors were obtained from the following references: GRB 970228: Galama *et al.* 2000; GRB 970508: Galama *et al.* 1999; GRB 971214: Diercks *et al.* 1998; GRB 980329: Reichart *et al.* 1999, Yost *et al.* 2002; GRB 980613: Hjorth *et al.* 2002; GRB 980703: Vreeswijk *et al.* 1999; GRB 990123: Castro-Tirado *et al.* 1999; Holland *et al.* 2000; GRB 990712: Sahu *et al.* 2000; GRB 991208: Galama *et al.* 2000, Castro-Tirado *et al.* 2001; GRB 000418: Klose *et al.* 2000, Gorosabel *et al.* 2003a (host) GRB 000926: Harrison *et al.* 2001, Castro *et al.* 2003; GRB 001011; Gorosabel *et al.* 2002; GRB 010222 Galama *et al.* 2003; GRB 011121; Greiner *et al.* 2003; GRB 020305: Gorosabel *et al.* 2005; GRB 020405: Masetti *et al.* 2003; GRB 020813: Covino *et al.* 2003, Gorosabel *et al.* 2002 (host)